Tunable complex-valued multi-tap microwave photonic filter based on single silicon-on-insulator microring resonator

Juan Lloret,[1,*] Juan Sancho,[1] Minhao Pu,[2] Ivana Gasulla,[1] Kresten Yvind,[2] Salvador Sales,[1] and José Capmany[1]

[1]*ITEAM Research Institute, Optical and Quantum Communications Group, Universidad Politécnica de Valencia, Camino de Vera s/n,46022 Valencia, Spain*
[2]*DTU Fotonik, Department of Photonics Engineering, Technical University of Denmark, Build. 343, DK-2800 Kongens Lyngby, Denmark*
[*]*jualloso@iteam.upv.es*

Abstract: A complex-valued multi-tap tunable microwave photonic filter based on single silicon-on-insulator microring resonator is presented. The degree of tunability of the approach involving two, three and four taps is theoretical and experimentally characterized, respectively. The constraints of exploiting the optical phase transfer function of a microring resonator aiming at implementing complex-valued multi-tap filtering schemes are also reported. The trade-off between the degree of tunability without changing the free spectral range and the number of taps is studied in-depth. Different window based scenarios are evaluated for improving the filter performance in terms of the side-lobe level.

©2011 Optical Society of America

OCIS codes: (070.1170) Analog optical signal processing; (130.3120) Integrated optics devices; (230.5750) Resonators.

References and links

1. A. Seeds, "Microwave photonics," IEEE Trans. Microwave Theory Tech. **50**(3), 877–887 (2002).
2. J. Capmany and D. Novak, "Microwave photonics combines two worlds," Nat. Photonics **1**(6), 319–330 (2007).
3. J. Capmany, B. Ortega, D. Pastor, and S. Sales, "Discrete-Time Optical Processing of Microwave Signals," J. Lightwave Technol. **23**(2), 702–723 (2005).
4. J. Yao, "Microwave Photonics," J. Lightwave Technol. **27**(3), 314–335 (2009).
5. J. Capmany, B. Ortega, and D. Pastor, "A Tutorial on Microwave Photonic Filters," J. Lightwave Technol. **24**(1), 201–229 (2006).
6. J. Long, C. Li, W. Cui, J. Huangfu, and L. Ran, "A Tunable Microstrip Bandpass Filter With Two Independently Adjustable Transmission Zeros," IEEE Microw. Wirel. Compon. Lett. **21**(2), 74–76 (2011).
7. W.-S. Chang and C.-Y. Chang, "Novel Micostrip Periodic Structure and Its Application to Microwave Filter Design," IEEE Microw. Wirel. Compon. Lett. **21**(3), 124–126 (2011).
8. A. Vélez, F. Aznar, M. Durán-Sindreu, J. Bonache, and F. Martín, "Tunable coplanar waveguide band-stop and band-pass filters based on open split ring resonators and open complementary split ring resonators," IEE Proc. Microwaves, Antennas Propag. **5**(3), 277–281 (2011).
9. V. Sekar, M. Armendariz, and K. Entesari, "A 1.2-1.6-GHz Substrate-Integrated-Waveguide RF MEMS Tunable Filter," Accepted in IEEE Trans. Microwave Theory Tech. (to be published).
10. W. Shen, W.-Y. Yin, and X.-W. Sun, "Compact Substrate Integrated Waveguide (SIW) Filter with Defect Groud Structure," IEEE Microw. Wirel. Compon. Lett. **21**(2), 83–85 (2011).
11. R. W. Boyd and D. J. Gauthier, "Slow and fast light," Prog. Optics **43**, 497–530 (2002).
12. T. F. Krauss, "Why do we need slow light?" Nat. Photonics **2**(8), 448–450 (2008).
13. S. Sales, W. Xue, J. Mork, and I. Gasulla, "Slow and Fast Light Effects and their Applications to Microwave Photonics using Semiconductor Optical Amplifiers," Trans. Microwave Theory and Tech J. Lightwave Technol. **58**(11), 3022–3038 (2010).
14. W. Xue, S. Sales, J. Capmany, and J. Mork, "Wideband 360° microwave photonic phase shifter based on slow and fast light in semiconductor optical amplifiers," Opt. Express **18**(6), 6156–6163 (2010).
15. L. Thévenaz, "Slow and fast light in optical fibers," Nat. Photonics **2**(8), 474–481 (2008).
16. S. Chin, L. Thévenaz, J. Sancho, S. Sales, J. Capmany, P. Berger, J. Bourderionnet, and D. Dolfi, "Broadband true time delay for microwave signal processing, using slow light based on stimulated Brillouin scattering in optical fibers," Opt. Express **18**(21), 22599–22613 (2010).
17. T. Baba, "Slow Light in Photonic Crystals," Nat. Photonics **2**(8), 465–473 (2008).

18. M. Patterson, S. Hughes, S. Combrié, N. V. Tran, A. De Rossi, R. Gabet, and Y. Jaouën, "Disorder-induced coherent scattering in slow-light photonic crystal waveguides," Phys. Rev. Lett. **102**(25), 253903 (2009).
19. D. B. Adams and C. K. Madsen, "A novel Broadband Photonic Phase Shifter," J. Lightwave Technol. **26**(15), 201–229 (2008).
20. M. Pu, L. Liu, W. Xue, Y. Ding, L. Hagedorn-Fradsen, H. Ou, K. Yvind, and J. M. Hvam, "Tunable Microwave Phase Shifter based on Silicon-on-Insulator Microring Resonator," Photon. Technol. Lett. **22**(12), 869–871 (2010).
21. M. Pu, L. Liu, W. Xue, Y. Ding, H. Ou, K. Yvind, and J. M. Hvam, "Widely tunable microwave phase shifter based on silicon-on-insulator dual-microring resonator," Opt. Express **18**(6), 6172–6182 (2010).
22. W. Xue, S. Sales, J. Mork, and J. Capmany, "Widely Tunable Microwave Photonic Notch Filter Based on Slow and Fast Light Effects," Photon. Technol. Lett. **21**(3), 167–169 (2009).
23. J. Sancho, S. Chin, M. Sagues, A. Loayssa, J. Lloret, I. Gasulla, S. Sales, L. Thévenaz, and J. Capmany, "Dynamic Microwave Photonic Filter Using Separate Carrier Tuning Based on Stimulated Brillouin Scattering in Fibers," Photon. Technol. Lett. **22**(23), 1753–1755 (2010).
24. M. Sagues, R. García Olcina, A. Loayssa, S. Sales, and J. Capmany, "Multi-tap complex-coefficient incoherent microwave photonic filters based on optical single-sideband modulation and narrow band optical filtering," Opt. Express **16**(1), 295–303 (2008).
25. F. J. Harris, "On the Use of Windows for Harmonic Analysis with the Discrete Fourier Transform," Proc. IEEE **66**(1), 51–83 (1978).

1. Introduction

Microwave Photonics (MWP) is currently an active area of research [1,2] as it enables the generation, transport and processing functionalities of radio frequency (RF), microwave and millimeter-wave signals directly in the optical domain [3,4]. MWP brings a series of advantages as compared to electronic technologies in terms of bandwidth, tunability, reconfigurability and electromagnetic interference (EMI) immunity.

One of the applications that has focused significant efforts within the MWP field is the implementation of flexible filters free from bandwidth constraints [5]. Although the electronic-based designs report high performance in terms of cost, quality factor (Q-factor) and stop-band rejection, they usually cannot offer wideband responses with high reconfigurability [6–10]. The most common electronic technology platforms used to implement filtering tasks are mainly based on microstrip [6,7], coplanar (CPW) [8] and substrate integrated waveguides (SIW) [9,10].

Aiming at developing accurate MWP based filtering schemes, the efficient design of broadband tunable microwave phase shifters and tunable true time delay lines is of key importance [5]. For this purpose, the exploitation of Slow and Fast Light (SFL) effects, which refers to as the capability of controlling the group velocity of light in certain media [11], represents a very promising alternative [12]. Several approaches spanning different technology platforms have already been demonstrated for the implementation of tunable phase shifting and true time delaying functionalities [13–21]. Among them, impressive results have already been reached in solutions based on semiconductor waveguides [13,14], nonlinear effects in optical fibers [15,16], photonic crystal (PhC) waveguides [17,18] and silicon-on-insulator (SOI) microring resonators (MRR) [19–21]. Concerning semiconductor waveguides, a notch-type filter at 30 GHz with 100% fractional tuning without changing the shape of the spectral response over a 30 MHz bandwidth has already been demonstrated [22]. The exploitation of nonlinear effects in optical fibers has led to adjustable free spectral range (FSR) and tunability [23]. However, this technology is bandwidth-limited and it is very difficult to integrate [23]. To the best of our knowledge, PhC-based MWP filtering schemes has not already been demonstrated.

The solutions suitable for being assembled in integrated on-chip devices are of strategic importance, because they can benefit from potential low cost, reliability and economics of scale. In this paper, a novel MWP filtering scheme based on single SOI MRR is presented and demonstrated. Tunability is accomplished by exploiting the phase-shift feature provided by the SOI MRR in combination with using optical single-sideband (OSSB) modulation in order to implement complex-valued taps. The tuning control mechanism is based on the fine adjustment of the different emission wavelengths instead of thermo-optical effects, as reported in [20-21]. The impact of the number of taps on the degree of tunability is deeply characterized. Finally, the fact of applying different windowing functions is analyzed in terms

of side-lobe level (SLL). The technique of combining OSSB modulation with passive optical filtering to implement complex-valued filters was originally proposed in [24], where phase shifters based on fiber Bragg gratings (FBG) instead of SOI MRR were considered.

2. Experimental setup and principle of operation

Figure 1(a) sketches the experimental setup of the MRR-based MWP filter. The approach implements a finite impulse response (FIR) filter, in which a number of taps N are generated by using an array of optical sources comprised of N distributed feedback (DFB) lasers operating in continuous wave (CW). The input RF signal $s_{in}(t)$ is imprinted on all the N optical carriers by means of a Mach-Zehnder modulator (MZM) in dual-drive configuration, giving as a result OSSB modulation. The N modulated optical signals are then sampled by an arrayed waveguide grating (AWG), which is featured by a channel spacing of 0.8 nm. This fact limits the emission wavelength of the N CW DFB lasers. Each sample is independently delayed via propagating through different optical delay lines. The delay difference between all the samples is known as basic delay (T), value which is inversely proportional to the FSR. All the samples are combined again, amplified using an erbium doped fiber amplifier (EDFA) and injected into the MRR. The samples are then weighted and phase shifted according to the MRR transfer function, which is shown in Fig. 1(b). Finally, the optical signal coming from the MRR output is photodetected and acquired by a vectorial network analyzer (VNA). In such a way, at the photodetector (PD) output the RF signal $s_{out}(t)$ is composed of the interference of all the N weighted, delayed and phase shifted samples.
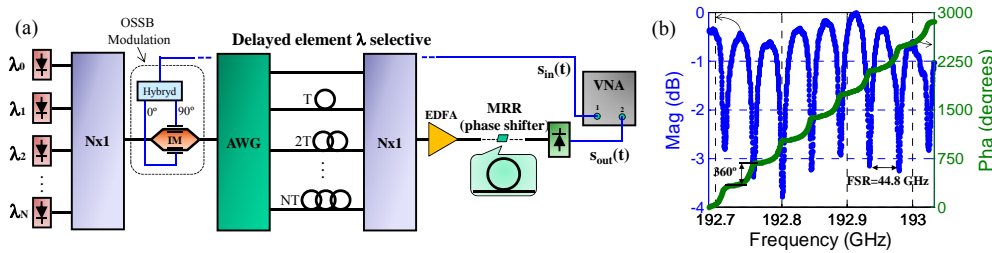

Fig. 1. (a) Experimental setup. (b) MRR magnitude and phase transfer functions.

The electrical transfer function of a FIR filter can be expressed as [5]

$$H(f) = \sum_{r=0}^{N-1} a_r e^{-j2\pi frT} = \sum_{r=0}^{N-1} |a_r| e^{jr\varphi} e^{-j2\pi frT},$$ (1)

where a_r denotes the complex-coefficient filter taps, f the RF frequency, T the basic delay and ϕ the basic phase shift. Attending to the setup depicted in Fig. 1(a), T is determined by the time spacing between adjacent samples, being in this case $T = 5.8$ ns. This fact yields a periodic spectral characteristic with a FSR approximately equal to 171 MHz in our setup.

The moduli of a_r are modified by the MRR, MZM and AWG transfer functions, as well as by the couplers and delay lines losses. It must be noticed that $|a_r|$ can be controlled by adjusting the emission power of the r-th CW DFB laser. This fact allows the implementation of windowed samples.

Exploiting the optical phase feature of the MRR (see Fig. 1(b)), the ϕ can be tuned by properly choosing the spectral placement of each of the N optical carriers. The 250 μm radius MRR was fabricated in a SOI wafer with a top silicon thickness of 250 nm and 3 μm buried silicon dioxide. The waveguide width is 450 nm. Tapered input and output ports are implemented to improve the fiber-to-chip coupling efficiency. The effective group index of the SOI waveguides is 4.26, which corresponds to a FSR of 44.83 GHz. The width and depth of the periodic response notches are determined by the coupling ring-to-waveguide gap, which is 200 nm. It must be noticed that a 2π phase shift occurs at each filter notch.

The center frequency of the MWP filter is limited by the optical phase transfer function of the MRR. In particular, the abruptness of the phase slopes establishes the minimum RF frequency able to obtain the maximum phase shift between an optical carrier and its modulation sideband. Attending to this fact, a center frequency of 20 GHz has been chosen. Zero phase unbalance between the minimum and maximum frequencies along the filter bandwidth is required to avoid the degradation due to distortion in the filter transfer function. This is the reason why the bandwidth has been limited to 1 GHz, i.e. f spans from 19.5 GHz to 20.5 GHz.

Proof-of-concept implementations involving $N = 2$, 3 and 4 samples have been considered. However, the design can be extrapolated to any arbitrary number of samples.

3. Results

3.1 Filter response

The suitability of the proposed scheme for implementing complex-valued coefficients is first demonstrated. The phase of the r-th sample, denoted by the term $r\phi$ in Eq. (1), is given by the phase shift between the r-th optical carrier and its corresponding sideband. In this manner, the mechanism for phase synthesis of the r-th sample focuses on the proper adjustment of the r-th CW DFB laser emission wavelength, in accordance to the MRR optical phase transfer function (see Fig. 2). By exploiting the MRR periodical phase response, the phase shifts are independently implemented for all the two, three and four coefficients designs respectively, a feature which is required in a multi-tap complex-valued tunable MWP filter. Figure 2 shows the spectral placement of the optical carriers when considering the four-tap implementation on the MRR optical phase response. The optical carriers and the 1 GHz bandwidth sideband range are represented for all the four samples. Figure 2(a) shows the scenario in which the phase difference between carrier and sideband of each sample is the same and minimum. In contrast, Fig. 2(b) shows the samples spectral placement when ϕ is the maximum and equal to 90°.

The MRR optical phase transition shape limits the total RF phase shift. As a function of the number of resonances in consideration, i.e. the number of samples, the minimum and maximum values of ϕ are changed. In case of using four taps, maximum phase excursion from 51° to 321° can be synthesized at a f of 20 GHz, yielding $\phi = 90°$ (see the insets of Fig. 2).
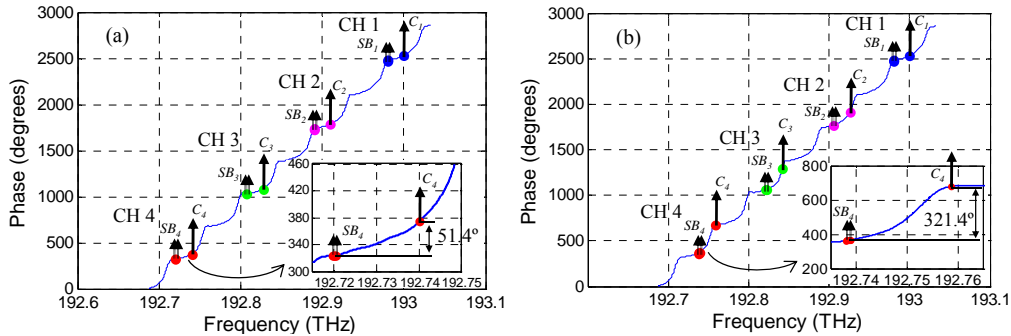

Fig. 2. Samples spectral placement on the MRR phase response for (a) minimum and (b) maximum filter tunability when $N = 4$.
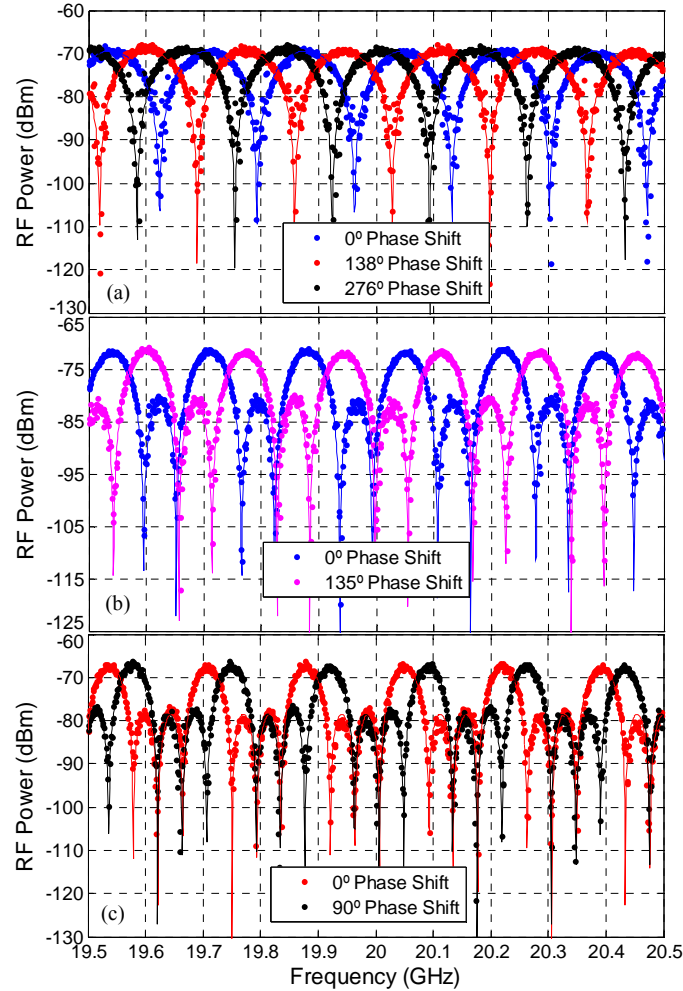
Fig. 3. Frequency response of the (a) two-tap, (b) three-tap and (c) four-tap complex-valued filter.

Figure 3 displays the filter frequency responses for three different approaches involving two, three and four complex-valued taps. Experimental (symbols) and theoretical (solid lines) results show good agreement. Small deviations are attributed to reflections in the electrical part of the setup and the residual unwanted sideband in the OSSB modulation. Rectangular (uniform) based windows have been used for all the three different approaches. Depending on the number of taps, different degrees of filter tunability have been achieved. In case of using two coefficients, a maximum phase shift excursion of 276° has been obtained. Figure 3(a) shows the notch-type filter response, leading to a continuously 77% fractional tuning. Three and four-tap based filter responses experiencing 38% and 24% fractional tunings can be seen in Fig. 3(b) and Fig. 3(c) respectively. In both cases, the maximum phase shift excursion has been 270°. Ideally, fractional tunings following $FSR/(N-1)$ could be reached. However, zero minimum RF phase shift cannot be obtained in practice. That is the reason why fractional tunings of the 100%, 50% and 33% have not been achieved when implementing the two, three and four-tap approaches respectively. As expected from Eq. (1), measurements corroborate that the FSR and the shape of the filter are not altered when its frequency response is tuned. The use of cascaded MRRs represents a suitable solution to enhance the fractional tuning. In particular, by cascading k identical MRRs, the maximum basic phase shift can be extended by a factor of k.

3.2 Windowing

Windowed samples have been demonstrated so far to reduce the undesirable effects related to spectral leakage in harmonic processing systems [25]. Within the filtering field, a considerable variety of windows have been evaluated [25]. Different performance improvements have been obtained in terms of selectivity and SLL according to the window features [25].
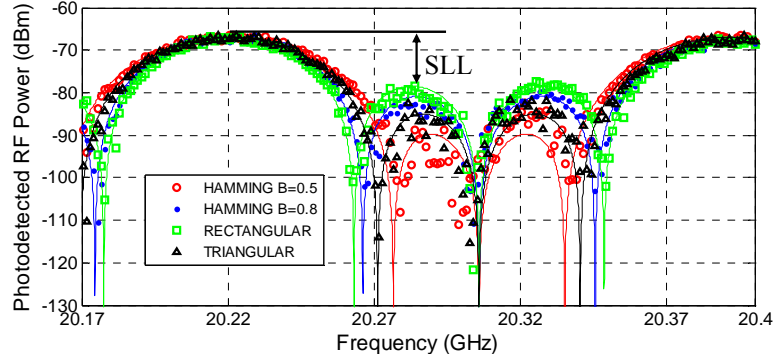

Fig. 4. Filter response as a function of the window.

Figure 4 shows the numerical and experimental results for the four-tap filter response when applying four different kinds of windows. Good agreement between calculated data and measurements can be seen. Specifically, rectangular, triangular and hamming based windows have been studied. In the case of the hamming window, two different values of the B-parameter have been considered [25]. In particular, no changes in the approach scheme are required and window samples can be readily accomplished acting on the emission power of the N CW DFB lasers. Results show an SLL improvement by more than 12 dB when considering the hamming window with B = 0.5 regarding the uniform window based scenario. The best selectivity is obtained by using the rectangular window. However, the out-of-band rejection level given by the SLL is the lowest. On the other hand, the maximum performance attending to the SLL is obtained by the hamming window with B = 0.5, but it is characterized by the worst selectivity. The hamming with B = 0.8 and triangular windows establish intermediate cases. Hence, improvements on both the selectivity and the SLL cannot be simultaneously obtained and the choice of using a certain window is application-dependent.

4. Conclusions

A novel tunable complex-valued multi-tap microwave photonic filter based on single SOI MRR has been proposed and demonstrated. Filter response tunability without changing the FSR can be accomplished by properly setting the emission wavelength of the N CW DBF lasers. The trade-off between the filter selectivity, given by the number of samples N, and the degree of tunability has been studied in-depth. Fractional tuning greater than 77% has been obtained when implementing two taps, whereas in the case of four taps it has been above 24%. These fractional tunings can be enhanced by using cascaded MRRs. The performance in terms of SLL can be just improved by properly engineering window based samples. Different window taps schemes have been evaluated. In particular, the hamming window with B = 0.8 has yielded the maximum SLL levels, rising up to 23 dB.